Q. J. R. Meteorol. Soc. (2003), **129**, pp. 2949–2969 doi: 10.1256/qj.03.08

Water vapour line and continuum absorption in the thermal infrared—reconciling models and observations

By JONATHAN P. TAYLOR*, STUART M. NEWMAN, TIM J. HEWISON and ANDREW McGRATH
Met Office, Bracknell, UK

(Received 8 January 2003; revised 25 June 2003)

SUMMARY

High-spectral-resolution thermal infrared radiance observations made with the Airborne Research Interferometer Evaluation System instrument on the Met Office C130 aircraft in tropical and sub-arctic atmospheres are used to evaluate the water vapour continuum and line absorption. Coincident microwave radiometer measurements at 183 GHz are used to help constrain the water vapour profile. Through careful selection of wavelengths where the water vapour continuum has varying impacts on the observed radiances, analysis shows that the continuum is too strong; this is using the General Line-by-line Atmospheric Transmittance and Radiance Model with the CKD2.4 water vapour continuum and High Resolution Transmission Molecular Absorption 2000 spectral database. Zenith observations from low altitude indicate that the continuum requires reducing by between 6% and 15% depending on the frequency, which is in good agreement with recent laboratory data. A modified continuum is presented and used in modelling to compare against upper-troposphere nadir measurements obtained in tropical and sub-arctic atmospheres.

KEYWORDS: Airborne ARIES HITRAN Spectroscopy

1. INTRODUCTION

Water vapour plays a critical role in meteorology and climatology, yet is one of the most difficult parameters to measure accurately, particularly its vertical distribution. The traditional and most widely used measure of water vapour is made with radiosondes, which are launched routinely by many national meteorological services.

Radiosondes give good vertical resolution but have poor global coverage because of the sparseness of the network. In particular, information about the vertical structure of temperature and water vapour over the ocean regions is not available from radiosonde observations. Global measurements of the vertical structure of temperature and water vapour are routinely made from satellite instruments, such as the High-resolution Infra-Red Sounder (HIRS; Smith *et al.* 1979) on the National Oceanic and Atmospheric Administration (NOAA) polar orbiting satellites, which has become the mainstay of infrared sounding from space. More recently microwave sounders have supplemented these infrared measurements. In 1998 the first Advanced Microwave Sounding Units (AMSU-A and AMSU-B) were launched on NOAA 15 and further instruments were launched on NOAA 16 in 2000 and NOAA 17 in 2002 (Goodrum *et al.* 2000). These instruments operate at a range of frequencies between 24 and 183 GHz. Their ability to sound through most of the clouds in the atmosphere is already benefiting operational numerical weather prediction (NWP; English *et al.* 2000) and further benefits are expected.

AMSU instruments represent a significant development in microwave sounding from space. Soon they will be complemented by developments in infrared sounding from space, which, although not being able to sound through clouds, will provide higher accuracy and greater vertical resolution in cloud-free conditions.

The first high-spectral-resolution thermal infrared instrument available for NWP will be the Atmospheric Infrared Sounder (AIRS; Aumann and Pagano 1994). This instrument was launched in March 2002 as part of the National Aeronautical and

* Corresponding author, present address: Met Office, FitzRoy Road, Exeter, Devon EX1 3PB, UK. e-mail: jonathan.p.taylor@metoffi ce.com

Space Administration (NASA) Earth Observing System Aqua mission. Although not an 'operational' platform, data from this instrument will be used by several NWP centres as a trial for the data due from the first operational high-resolution sounder in late 2005. The first operational high-spectral-resolution sounder giving frequent global coverage will be the Infrared Atmospheric Sounding Interferometer (IASI; Amato *et al.* 1995). This will fly on the European funded Meteorological Operational Satellite (METOP) which has a first launch due in December 2005. Further METOP satellites will follow this, and the Crosstrack Infrared Sounder will be its counterpart on the US National Polar orbiting Operational Environmental Satellite System, with a first launch due in 2009.

In preparation for these microwave and thermal infrared sounders the Met Office has installed microwave and infrared instrumentation on the Meteorological Research Flight (MRF) C130 aircraft. In 1989 the Met Office installed the Microwave Airborne Radiometer Scanning System (MARSS) which measures at the same frequencies as AMSU-B, and in 1995 a further microwave radiometer, Deimos, that measures at the same frequencies as AMSU-A. In 1997 the Met Office installed the Airborne Research Interferometer Evaluation System (ARIES) on the C130, which measures in the thermal infrared between 600 and 3000 cm^{-1} at a resolution of 0.5 cm^{-1} (maximum optical path difference of 1 cm). This instrument measures over the same spectral range as IASI. Over the last decade these instruments have been used in radiative transfer studies with the aim of improving our understanding of the data to be received from the new generation satellite sounders described above.

One aim of the research has been to assess the spectroscopy in the spectral ranges used by the new satellite instruments AMSU and IASI. During 1999 the Met Office conducted two field campaigns under the name of MOTH (Measurement of Tropospheric Humidity) to study radiative transfer in the AMSU and IASI spectral ranges. MOTH-Tropic was flown in the spring of 1999 based on Ascension Island in the tropical South Atlantic and MOTH-Arctic was flown in December 1999 based on Kalmar in the Baltic Sea in Northern Europe.

A detailed understanding of the spectroscopy and, importantly, the level of uncertainty, is required to fully utilize the data from the future high-resolution infrared sounders and assimilate these data into NWP models. These new sounders have many thousands of channels, and most NWP centres will select a subset of these for assimilation. Clearly it makes sense, where possible, to select channels where the uncertainty in the radiative transfer is a minimum.

In comparing a radiometric observation with a model there are several sources of uncertainty: instrument noise, model error, spectroscopy error, and representivity errors. A research aircraft has the advantage of being able to make *in situ* observations of the structure of the atmosphere in which the radiation measurements are made. However, the innate variability of the atmosphere means great caution needs to be taken in prescribing the state of the atmosphere for the model calculations that is representative of the radiance observations.

In this paper, we utilize both the microwave brightness temperature measurements and the high-spectral-resolution infrared radiance measurements made by the Met Office C130. The microwave radiometer brightness temperatures are compared with model simulations using detailed *in situ* measurements of the water vapour profile by aircraft and radiosondes. During a scientific sortie there are a range of observations of water vapour available: dropsondes, radiosondes and aircraft profiles up and down through the atmosphere. By minimizing the difference between microwave radiometer observations using models initialized with each of the possible profile options in turn, we are able

TABLE 1. THE CHARACTERISTICS OF THE MICROWAVE RADIOMETERS DURING MOTH

	MARSS[1]				
AMSU[2] channel	16	17	18	19	20
Centre frequency (GHz)	89.0	157.0		183.25	
IF[3] bandwidth (GHz)	1.3–3.9	1.3–3.9	0.75–1.2	2.5–3.5	6.0–8.0
Beam width (FWHM[4])	11.8°	11°		6.2°	
Scan period			3s		
Views		Nadir ± 40° and Zenith ± 40°			
Calculation accuracy (K)	0.9	1.1	1.0	0.9	0.8

[1] Microwave Airborne Radiometer Scanning System.
[2] Advanced Microwave Sounding Unit.
[3] Intermediate Frequency.
[4] Full Width Half Maximum.

to select our 'first-guess' observed profile that represents the atmosphere in which the radiance measurements were made. We then use the fact that the high-resolution infrared data from ARIES is able to discriminate window regions and water vapour lines of varying strength to further constrain the profile input to the models. As a result of this analysis we are able to identify evidence for uncertainties in the spectroscopy and modelling, such as errors in the strength of the water vapour continuum.

In section 2 a more detailed description of the instrumentation, in particular the radiometers, flown on the Met Office C130 aircraft is presented. Section 3 briefly presents details of the two MOTH campaigns. In section 4 the validation of the microwave radiometer measurements against state of the art radiation models is presented, followed in section 5 by comparisons of the infrared measurements with their respective radiation model. A discussion and conclusions follow in section 6.

2. AIRCRAFT INSTRUMENTATION

(*a*) *Microwave radiometers*

MARSS is a total power radiometer with channels at 89 and 157 GHz, and three channels centred on 183 GHz. Table 1 shows its characteristics during MOTH. It is described in more detail in McGrath and Hewison (2001).

Figure 1 shows the atmospheric absorption in this part of the spectrum for cold dry conditions in the mid-troposphere (550 hPa, 235 K, 0.1 g kg^{-1}). The lines identified in the legend show absorption predicted by a range of models: MPM89 (Liebe 1989), MPM93 (Liebe *et al.* 1993), Rosenkranz (Rosenkranz 1998), and CKD2.4.1. Clough *et al.* (1980, 1989) The spectrum shows a single oxygen resonant line at 118 GHz and a water vapour line at 183 GHz. The models are in good agreement near these lines, but diverge in the intervening 'window' regions, due to different representation of the water vapour continuum which dominates emission here; this is represented semi-empirically, and it is this component that differs most between models. Some differences can also be attributed to the wings of the 60 GHz oxygen complex at frequencies below 100 GHz.

The shaded areas in Fig. 1 represent the dual pass bands of each of the MARSS channels. The absorption measured by MARSS in these conditions is shown as crosses. Although MARSS measures the sum of both pass bands simultaneously, these are shown separately, linked by a horizontal bar for clarity.

MARSS observations are in good agreement with the model predictions near the centre of the 183 GHz line. However, all the models appear to be deficient in absorption

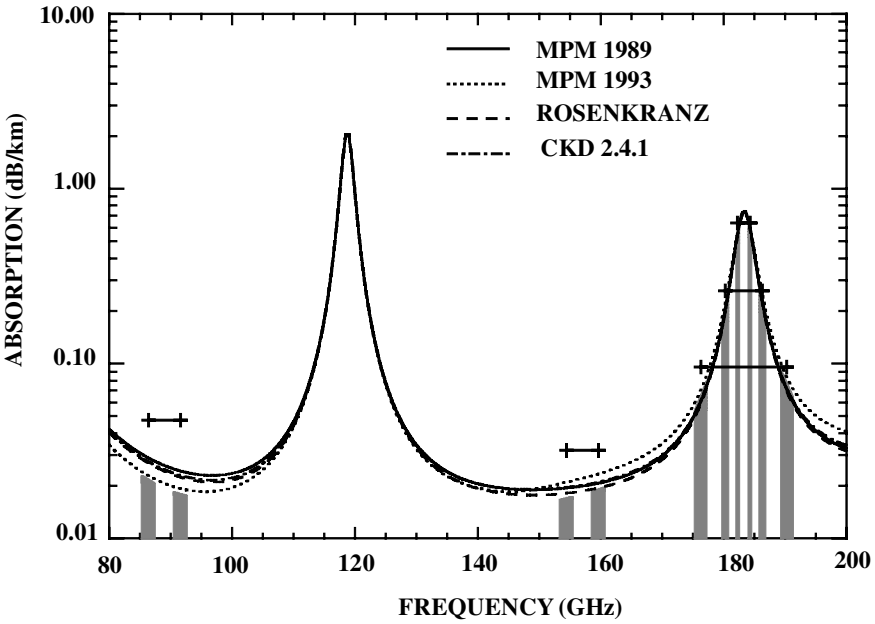

Figure 1. A spectrum of atmospheric absorption evaluated with a range of models identified in the text. The measurements from MARSS are shown as crosses.

in the window channels. This suggests the strength of the continuum absorption is underestimated by the models. The cause of this is the subject of another paper. For this study, only the well modelled 183 GHz channels are used to help constrain the choice of humidity profile used in the infrared radiative transfer.

(*b*) *Thermal infrared interferometer*

The ARIES instrument measures thermal radiation between 600 and 3000 cm^{-1}. It is a modified Bomem instrument with a maximum optical path difference of 1 cm; full details of the instrument specification and calibration are given in Wilson *et al.* (1999). In flight, the instrument is calibrated by two black body targets, one of which is heated whilst the other is at ambient temperature. In addition to viewing these targets, the interferometer can be commanded to view in the zenith, nadir and a range of angles between nadir and 60 degrees off nadir across track. In this paper, results from the zenith views at low level (30 m) looking up through the atmosphere and nadir views at high level (~8 km) looking down through the atmosphere will be presented.

(*c*) *Measurement of water vapour*

On the MRF C130 aircraft water vapour is measured using a total water hygrometer (TWC) which uses absorption in the Lyman-α band. This instrument was developed at MRF and has a rapid response of 64 Hz. In this analysis these data have been averaged to 1 Hz, which represents a horizontal distance of approximately 100 m, and during profiles a vertical resolution of between 2.5 and 5 m. In addition to this instrument a General Eastern dew-point hygrometer was operated. This instrument uses a chilled-mirror technique to determine the dew-point. However, the slow response of this instrument during profiles means that its use is restricted to calibrating the TWC measurement. During the MOTH campaigns the MRF C130 also dropped sondes. These dropsondes

fall from the aircraft to the ocean surface below a small parachute, and use an RD93 sensor that is based on a Vaisala RS90 radiosonde. They include a GPS receiver so that their position and the wind speed can be monitored in addition to measurements of the temperature and water vapour profiles. These dropsondes have the advantage that they fall fairly quickly at around 12 m s^{-1} allowing a fairly narrow column of atmosphere to be measured. Analysis of the dropsonde measurements during MOTH, comparing them with aircraft and radiosonde data, have shown that there is a systematic bias in the humidity measurement which is discussed in Vance *et al.* (2003). For this reason dropsonde data have not been used in this analysis.

During both MOTH campaigns, well-calibrated radiosondes were launched from islands in the vicinity of the flight trials. These radiosondes were a mixture of Vaisala RS80, Vaisala RS90 and Meteolabor Snow White sensors. A detailed intercomparison of these different measurements is the subject of another paper. The methodology adopted in choosing the most representative profile of water vapour for input into the radiative transfer models, using the information from the aircraft sensors and the radiosondes, is described in subsection 5(a).

3. The MOTH campaigns

During 1999, the Met Office conducted two MOTH experiments with the objective of measuring tropospheric humidity: MOTH-Tropic was based on Ascension Island in the South Atlantic during April and May, where integrated water vapour column amounts of from 29 to 42 kg m^{-2} were measured; MOTH-Arctic took place in the Baltic Sea during December, where the water vapour burden was much lower (as low as 4.1 kg m^{-2}). During MOTH-Tropic radiosondes were launched from Ascension Island (8°S, 14°W), and during MOTH-Arctic from Visby (57.6°N, 18.2°E) on the island of Gotland in the Baltic Sea.

Nine flights of the C130 were made in total specifically for MOTH experiments. Most flights started and ended with a climb from minimum to maximum altitude and a dropsonde launch close to the radiosondes' island launch site. This was followed by a transit to a nearby oceanic area thought to be clear of cloud, and another profile in the operating area. A stack of straight and level runs was then flown at various levels over a period of several hours. Dropsondes were again released during the high-level runs in the operating area.

Where possible, flights were timed such that the high-level runs in the operating area coincided with the sub-satellite track of a NOAA-15 overpass; this satellite carried the first AMSU instruments.

4. Microwave radiative transfer studies

Downwelling (zenith) radiances observed by MARSS during straight and level runs at all altitudes, were filtered to select only periods where the calibration was stable and skies above known to be clear. Data from these runs were then averaged for comparison with predictions from the MPM89 radiative transfer model, and others.

Radiosonde data from the nearest launch were used to 'top-up' the aircraft temperature and humidity profile to 20 hPa. Aircraft data from the total water probe, taken during a composite of profiles just before or after the runs, were used to generate the profile of water vapour between the surface and the aircraft maximum ceiling. These were then converted to humidity mass mixing ratio and re-sampled onto a 2 hPa vertical grid for input to the radiative transfer model to minimize sampling errors. The humidity mass

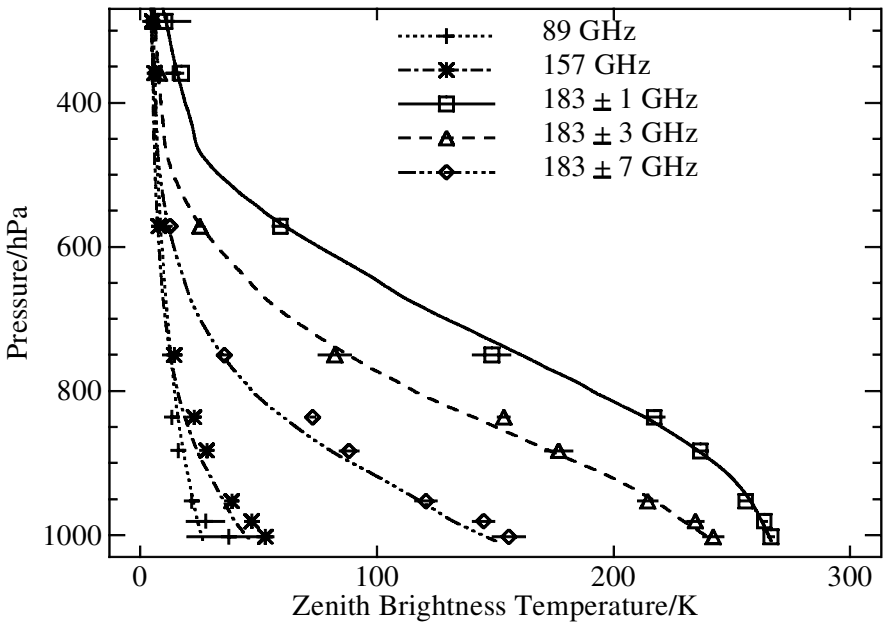

Figure 2. A comparison of MARSS measurements and simulations using the MPM-89 radiation model initialized with *in situ* aircraft profiles of temperature and humidity. See text for details.

mixing ratios are believed to be accurate to $< \pm 5\%$ at low levels, increasing to $< \pm 15\%$ above about 400 hPa (Ström *et al.* 1994).

Figure 2 shows the results of this comparison for the driest flight recorded during MOTH-Arctic—identified by the unique flight number A742. MARSS measurements are shown together with error bars that represent their estimated accuracy. The results show an encouraging level of agreement between all the models and the MARSS data, particularly for the channels centred around 183 GHz. For the rest of this work we concentrate on these 183 GHz channels and use the MPM89 model; the choice of model is not significant. In general, the observations were found to be in better agreement with the models for flights in more humid conditions, especially in the window channels.

5. Infrared radiative transfer studies

The exploitation of satellite data for NWP by the use of variational analysis schemes requires the rapid computation of radiances from input atmospheric profiles. To do this, a fast radiative transfer model is used; these have their heritage in more complete, and considerably slower, line-by-line models. NWP centres are not expecting to use all of the thousands of channels that will become available from instruments like AIRS and IASI—rather they will select channels that enable the accurate retrieval of profiles of temperature, water vapour and some other species. In preparation for IASI and AIRS the spectroscopy of water vapour in the thermal infrared needs evaluating. This has two major benefits: firstly, an understanding of where in the spectrum the uncertainties in the radiative transfer are the highest will give guidance on channel selection; secondly, by improving our understanding of the radiative transfer we will reduce the magnitude of the error characteristics in our forward models, allowing the true benefit from the observations to be seen in the variational retrieval scheme. In this study we validate the

spectroscopy of the High Resolution Transmission Molecular Absorption (HITRAN) 2000 database implemented in the GENLN2 v.4 (Edwards 1992) line-by-line model, against high-spectral-resolution measurements made with an airborne interferometer ARIES. GENLN2 is the line-by-line model being utilized in the development of the fast radiative transfer code, RTIASI. Both the Met Office and the European Centre for Medium-Range Weather Forecasting will be using RTIASI as their operational fast model for the assimilation of IASI radiances in to their respective NWP models.

We have shown that the MPM89 model gives good agreement with airborne observations in the microwave region of the electromagnetic spectrum around 183 GHz (AMSU channels 18, 19 and 20). Water vapour data are available from the aircraft's *in situ* sensors and radiosondes. The spatial and temporal variability in the vertical profile of water vapour means that, without care, errors in the specification of the profile will dominate any radiative transfer studies.

(*a*) *Selecting the first-guess profile*

The microwave brightness temperature observations, made with the MARSS radiometer, have been used to build the best first-guess representation of the temperature and water vapour profiles for a range of tropical and sub-arctic cases. The zenith-viewing microwave measurements from the highest-level aircraft run have been used to select the best radiosonde profile to top up the aircraft measurements, by minimizing the r.m.s. difference between the radiometer observations and the model predictions for the most sensitive channels around 183 GHz.

The best tropospheric profile from the aircraft data has been constructed by minimizing the differences over all 183 GHz channels using data from all heights flown between 30 m and around 7–9 km. These first-guess profiles have then been used to initialize the GENLN2 v4 line-by-line radiation model and compute the radiances at the aircraft flight level for each case.

The GENLN2 model (Edwards 1992) treats the water vapour continuum using the semi-empirical approach of Clough *et al.* (1980, 1989). The continuum absorption is normally attributed to two components: self- and foreign-broadening. The total absorption coefficient, at frequency υ, due to the self and foreign water vapour continuum is defined in Clough *et al.* (1989) as:

$$k(\upsilon) = \upsilon \tanh\left(\frac{hc\upsilon}{2kT}\right)\left\{\tilde{C}_{\mathrm{s}}^{0}\left(\frac{\rho_{\mathrm{s}}}{\rho_0}\right) + \tilde{C}_{\mathrm{f}}^{0}\left(\frac{\rho_0}{\rho_{\mathrm{f}}}\right)\right\},$$

where T is temperature, ρ_{s} is the self (H_2O) density, ρ_{f} the foreign (dry air) density and ρ_0 the standard-atmosphere density. $\tilde{C}_{\mathrm{s}}^{0}$ are the self-broadening coefficients and $\tilde{C}_{\mathrm{f}}^{0}$ the foreign-broadening coefficients, whilst h, c and k are the Planck constant, speed of light and Boltzmann constant, respectively.

In the CKD continuum of Clough *et al.* (1980, 1989) a different form of the self-broadening coefficient may be used, namely:

$$C_{\mathrm{s}}^{0} = \upsilon \tanh\left(\frac{hc\upsilon}{2kT}\right)\tilde{C}_{\mathrm{s}}^{0}\frac{T_0}{Tp_0},$$

where $T_0 = 296$ K and $p_0 = 1$ atmosphere. It is this form of the self-broadening coefficient that is considered in the rest of this paper. The self-broadening component is some three orders of magnitude larger than the foreign-broadening component in the region of interest here, and will be considered in isolation henceforth. Measurements of the water vapour continuum in the laboratory are hampered by the need for long path lengths—this gives the motivation for using an airborne platform.

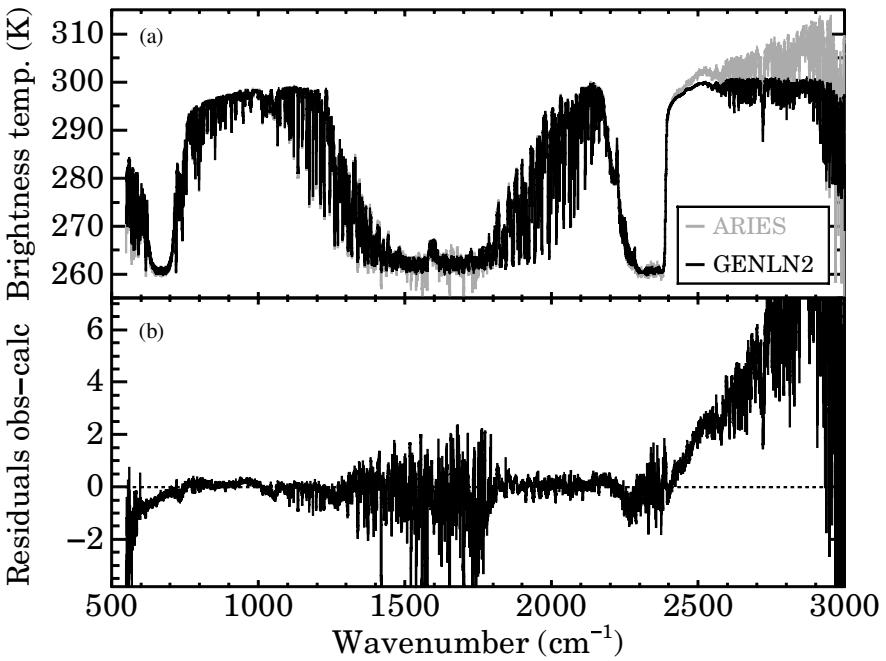

Figure 3. (a) A comparison of ARIES nadir brightness temperature observations (ten scans) at 7 km and a GENLN2 simulation for flight A670 in the tropics; (b) the residual brightness temperature difference of ARIES minus the GENLN2 model. See text for details.

In this work the CKD2.4 version of the water vapour continuum is used in conjunction with the HITRAN 2000 spectroscopic database*. An analysis of the difference between the HITRAN 96 and the HITRAN 2000 databases, and a comparison with aircraft observations are given in Newman and Taylor (2002). The authors are aware of the differences in the treatment of line centre absorption and continuum absorption with the CKD continuum and various line-by-line models, and this has been correctly treated in our simulations using GENLN2. The results from the model are compared with the radiances observed using the ARIES interferometer looking in the nadir and zenith. The ARIES instrument was mounted within an under-wing pod on the MRF C130 aircraft. The particularly strong carbon dioxide absorption features around 670 cm^{-1} and between 2300 and 2400 cm^{-1} are sensitive to the short atmospheric path inside the instrument pod. An estimate of the internal pod temperature is obtained from monitoring a platinum resistance thermometer mounted next to the ARIES scan mirror. Including a short path of approximately 0.3 m at this temperature in the model simulations reproduces the observed spectral features well.

All GENLN2 simulations presented in this work were first computed at a spectral resolution of 0.01 cm^{-1} and subsequently degraded to ARIES resolution, first by being passed through a Fourier transform and then by truncation of the resulting interferogram. During this process the instrument line shape of ARIES was also imposed on the modelled spectra allowing direct comparisons to be made.

Figure 3 shows an intercomparison between GENLN2 and measurements from the ARIES instrument for flight A670 that took place in the tropical South Atlantic on 28 April 1999. Figure 3(a) shows the ARIES nadir-viewing brightness temperature

* The HITRAN 2000 database can be downloaded from http://www.hitran.com

measurements taken at an altitude of 7 km as the lighter grey line, with the GENLN2 simulation shown as the dark line. The GENLN2 simulation was initialized using the first-guess profile, i.e. that constrained by the microwave radiometer data. The sea surface temperature was measured by ARIES during a run at 30 m altitude, approximately 60 minutes before the upper-level run over the same area. The sea surface temperature was 301.4 K and the spectral variation of the emissivity was modelled using that given by Masuda *et al.* (1988). Figure 3(b) shows the difference in brightness temperature: observations minus modelled.

Before more closely analysing the difference between the ARIES and modelled radiances, it is instructive to look at some of the larger-scale features of the radiance spectra presented. Looking at of Fig. 3(a) for reference, it can be seen that between 600 and 700 cm^{-1} the atmosphere has a very strong carbon dioxide absorption feature. In this region of the spectra ARIES is essentially sounding the temperature of the atmosphere immediately around the aircraft. This is also the case in the region of 2300 and 2400 cm^{-1}—another strong carbon dioxide absorption band.

Between 800 and 1200 cm^{-1} the absorption by water vapour is a minimum, and for this reason this range is often called the atmospheric window. There is, however, a significant ozone absorption band around 1000 cm^{-1} that needs to be represented within the model simulations. Between 1200 and 2100 cm^{-1} we have a region of variable water vapour absorption. In the middle of this region are some very strong water vapour lines that cause particular problems in the calibration of interferometers working in the relatively moist troposphere. For clarity these lines have been omitted in some of the figures.

Beyond 2400 cm^{-1} (i.e. as we move to shorter wavelengths) the ARIES instrument will measure not only the thermal emission of the atmosphere but also reflection of solar radiation: either Rayleigh, by aerosols or by the ocean surface. The GENLN2 line-by-line model does not allow for the computation of the solar component, and this accounts for the growing difference between the model and measured brightness temperatures between 2500 and 3000 cm^{-1}, evident in Fig. 3.

Taking these instrument and model deficiencies into account, it can be seen from Fig. 3(b) that the model and observations agree to within ± 1 K across almost the entire spectrum and in many places agreement is considerably better than this.

Figure 4 shows ARIES observations from the same flight, A670, but here ARIES is looking in the zenith at an altitude of 30 m above the tropical ocean surface. The observations are compared with a GENLN2 simulation of the downwelling brightness temperature. The very large differences above 2400 cm^{-1} are due to the solar component not being modelled in GENLN2. When looking in the zenith there is no warm emitting surface, and hence the radiance observed is critically dependent on the atmospheric absorption and emission. Figure 5 shows the same data but covering the window region only. In this region the contribution from the water vapour continuum is more dominant and a zenith view represents a very rigorous test of the continuum formulation.

Before drawing conclusions on the errors in a radiation model the inherent noise characteristics of the instrument must first be accounted for. The ARIES instrument measures radiance, and this changes by several orders of magnitude between 500 and 3000 cm^{-1}. Consequently, when converting to brightness temperature using the Planck function, a small difference, ΔR, in radiance can equate to a significantly different ΔT, depending on the wave number at which the measurement is made. In order to recognize this, it is important to understand what the intrinsic noise levels are for an interferometer like ARIES, and to consider whether the difference observed between an observation

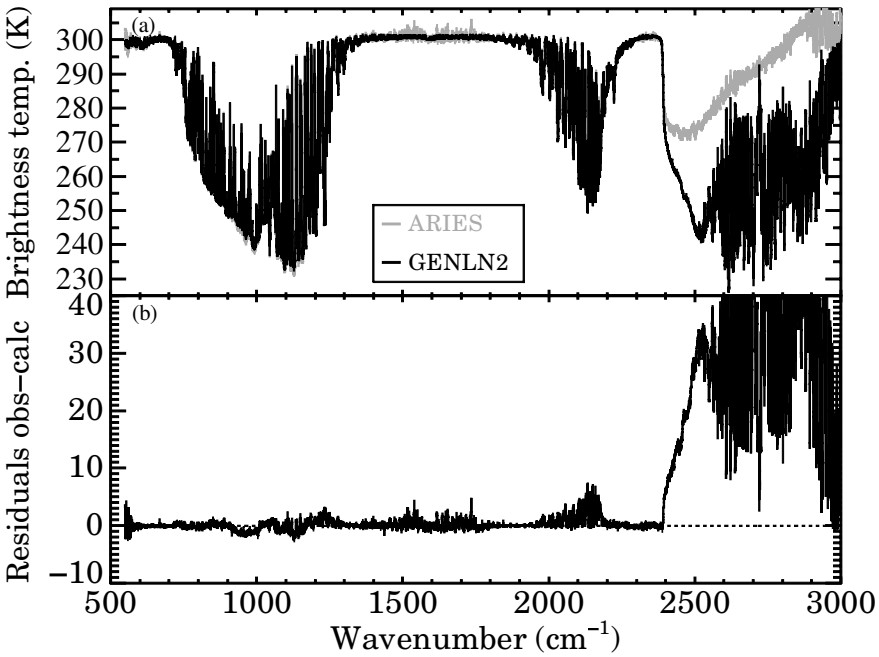

Figure 4. (a) A comparison of ARIES observations and GENLN2 simulations for a zenith view from 30 m altitude above the ocean during flight A670; (b) the brightness temperature difference ARIES minus GENLN2. See text for details.

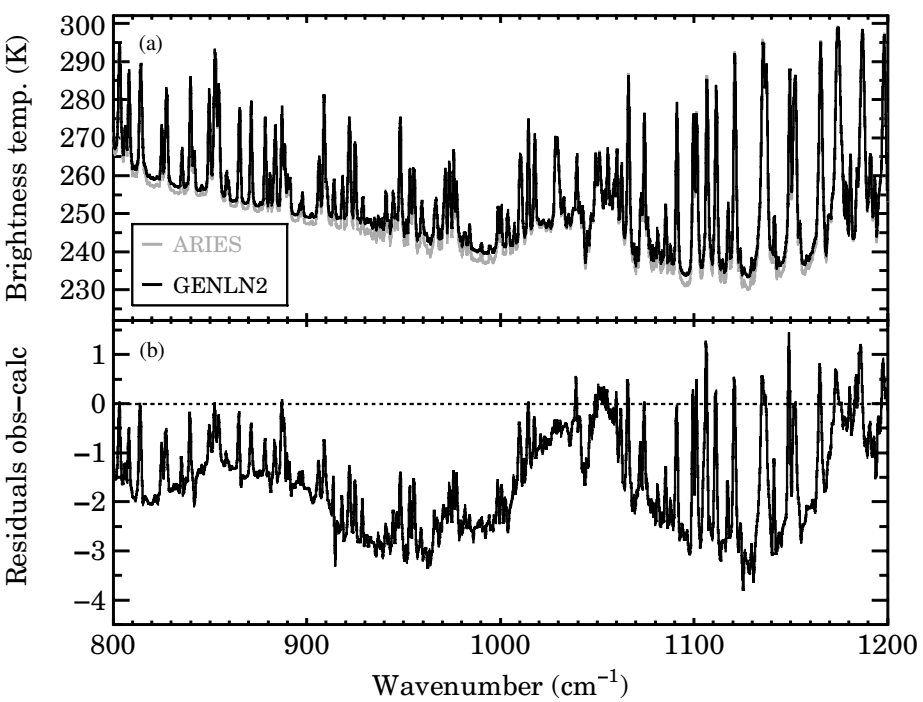

Figure 5. As Fig. 4 but zoomed in over the infrared atmospheric window region.

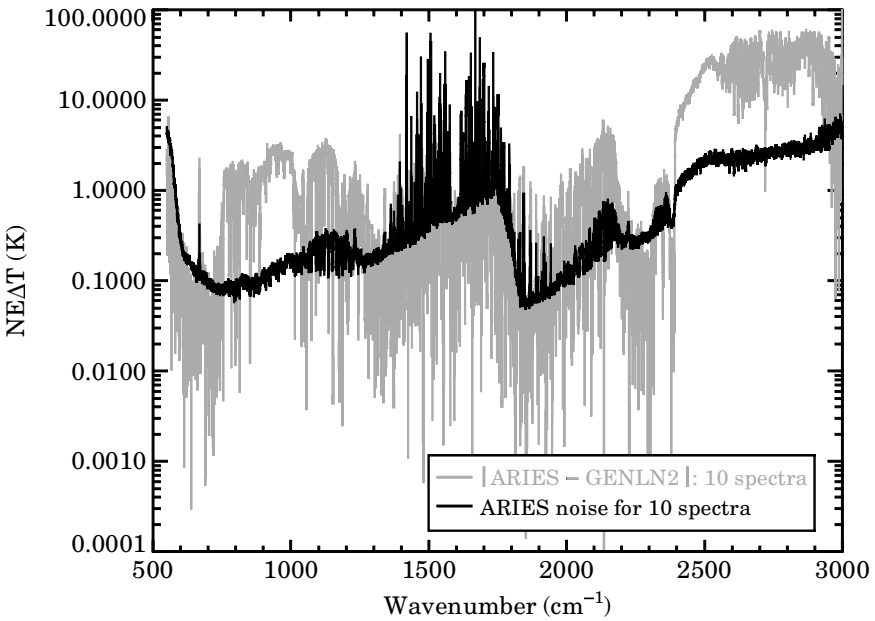

Figure 6. The absolute magnitude of the difference between the ARIES observations and GENLN2 for the case shown in Fig. 4 (light grey line) and the expected noise of ARIES (solid line) based on laboratory measurements.

and a model result lies above the noise level; the noise of the ARIES instrument was measured and described in Wilson *et al.* (1999). The technique consists of looking at a thermally stable external black body target and recording multiple interferograms—each interferogram being stored independently. After calibration against the instrument's internal black body targets the standard deviation of the real part of the radiance spectra of the multiple views of the external black body target can be evaluated to give the noise-equivalent radiance $NE\Delta R$. The noise-equivalent brightness temperature can then be evaluated at any particular temperature using the relationship:

$$NE\Delta T = \frac{NE\Delta R}{\mathrm{d}R/\mathrm{d}T}$$

where $\mathrm{d}R/\mathrm{d}T$ is the differential of the Planck function, evaluated at the temperature of interest.

The impact of instrument noise on a measurement can be decreased by averaging several interferometer spectra gathered sequentially whilst looking at a stable target. The interferometer instrument noise is inversely proportional to the square root of the number of interferometer scans co-averaged. In the real atmosphere the scene is rarely stable, so a balance has to be drawn between averaging spectra to reduce noise and introducing variability in the radiance due to the changing scene. In Fig. 6 the brightness temperature difference for ARIES minus the GENLN2 simulation for the zenith view in flight A670 (see Fig. 5) is plotted as the light grey line. In this figure the absolute value of the difference between observation and model is presented to facilitate the use of a log axis on the ordinate and direct comparison with the expected level of instrument noise. In taking the ARIES measurement ten spectra have been co-averaged, which equates to a time interval of 3 seconds or approximately 300 m of horizontal flight.

Figure 6 also shows the ARIES instrument noise expected for ten co-averaged spectra as the dark line. In computing this noise figure the laboratory derived $NE\Delta R$ has

been divided by dR/dT evaluated at each wave number at the brightness temperature of the observation. In this manner we are able to see how the fixed $NE\Delta R$, associated with the instrument system, manifests itself on an observed brightness temperature spectrum.

The 'W' shape of the instrument noise curve arises from the fact that the radiance spectrum is generated from two detectors that intersect at around 1750 cm^{-1}. Towards the edge of the detectors' sensitivity ranges the noise increases. Around the 1500–1800 cm^{-1} spectral region there are several strong water vapour absorption lines. The absorption by these lines is very strong, and causes problems in the calibration of the ARIES instrument at these spectral features. Because ARIES is operated in the troposphere or lower stratosphere where there is considerable water vapour, absorption can occur in the short path length between the external calibration targets and the enclosed interferometer. Such absorption cannot be corrected for in the calibration process and, since the properties of this short path can change in time, the result can be spurious spikes in the radiance spectra. Such features will of course not be an issue for space-borne instruments. In Fig. 6 it can be seen that in the window region, between 800 and 1200 cm^{-1} the difference between observation and model clearly exceeds the instrument noise by approximately an order of magnitude. In other spectral regions the difference between observations and model simulations is close to or, indeed, less than the expected noise based on laboratory measurements. Where the difference is less than the laboratory-based noise we cannot expect to comment on the suitability of the model or the spectroscopic database. The shape of this brightness temperature difference in the window region is consistent with an error in the water vapour continuum (Han *et al.* 1997). Furthermore, these observations suggest that the continuum is too strong, which is in agreement with the recent laboratory results of Cormier *et al.* (2002) who suggests that the self-broadening coefficients of the water vapour continuum need to be reduced by around 12%. Cormier's results are restricted to the three wavelengths at which he and co-workers were able to make laboratory measurements (931.002, 944.195 and 969.104 cm^{-1}), which fall within the spectral range in question here.

(*b*) *Assessment of the water vapour continuum*

We have set out to investigate whether the water vapour continuum used in GENLN2, in this case the CKD2.4 continuum can be improved. However, in addition to possible errors in the continuum there may be errors in the definition of the atmospheric profile input into the line-by-line model that could account for the observed differences. At this stage the GENLN2 model has been run using our first-guess profile as detailed above. Although the microwave radiometer measurements have helped us constrain the profile, there is still scope for errors in the water vapour in this profile of up to 10%, which is the constraint of the absolute accuracy of the microwave radiometer data.

ARIES has the advantage of making simultaneous radiance observations at a fairly high spectral resolution of around 0.5 cm^{-1}. Here we utilize this capability to study the errors associated with the profile. The first stage is to find spectral features in the ARIES observations that are dominated by the water vapour line absorption and are relatively insensitive to the water vapour continuum.

GENLN2 has been run using the first-guess profile with and without the water vapour continuum being accounted for, to predict the downwelling radiances at 30 m (i.e. the flight conditions for Fig. 5). Since we are expecting the error in the continuum to be no more than 10% (based on the results of Cormier *et al.*), spectral points have been selected where the difference between the continuum and no-continuum model runs were less than 1 K, a 10% error in 1 K being easily within the detectability range of ARIES. The selection of these spectral points was further constrained by ensuring:

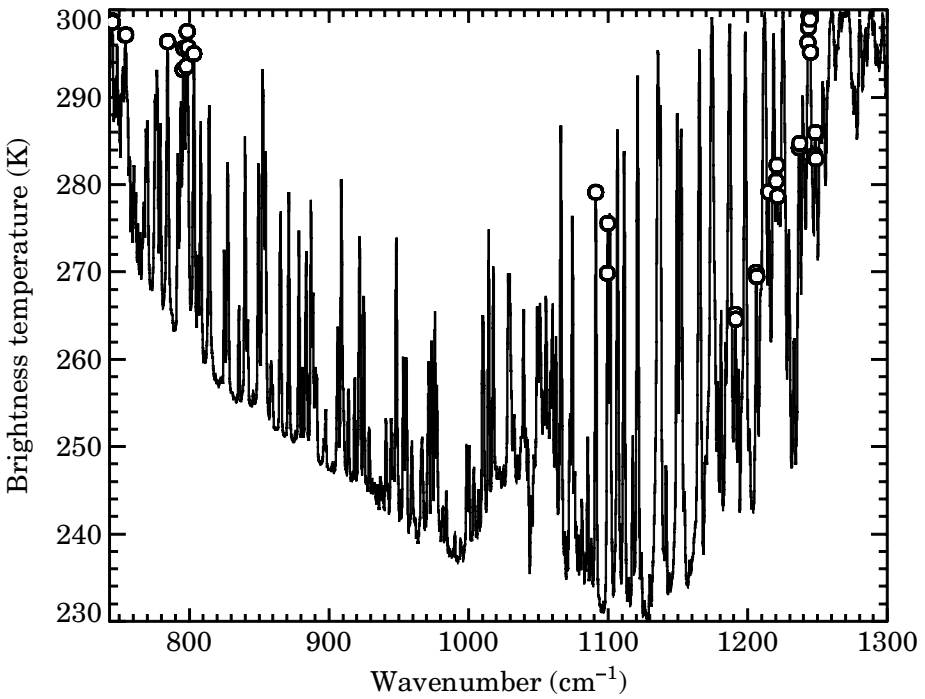

Figure 7. The downwelling brightness temperature, as measured by ARIES, at 30 m altitude during flight A670. The circles identify the 'channels' chosen as those where the water vapour continuum is at a minimum. See text for details.

(i) that the only significant absorber was water vapour; (ii) that the spectroscopy is well known, i.e. only including points where the differences could be explained by realistic perturbations to the water vapour profile; and (iii) that the selected spectral points are sensitive to the water vapour at a range of altitudes.

The result was that 32 spectral points were identified where the impact of the continuum is a minimum and where the lines dominate, and hence they are sensitive to the vertical structure of the water vapour profile. These points are shown as circles in Fig. 7, which presents the observed brightness temperature as a function of wave number. The brightness temperatures associated with the 32 points range from 264 to 300 K showing sensitivity to a range of different altitudes; in particular to the lower levels where the water vapour is a maximum.

Having selected these points where the impact of the continuum formulation is a minimum, GENLN2 has been run several times, and the brightness temperature evaluated at the 32 spectral points with the water vapour column increased and decreased uniformly by increments of 1% spanning the range -10 to $+10$%. By looking at the sensitivity of these model runs, the percentage change in the water vapour column (at all levels) required to force agreement between GENLN2 and ARIES for each of the 32 points has been computed. These required changes in water vapour column are shown in Fig. 8.

In Fig. 8 the average change required, over all 32 channels, is shown as the solid line ($+0.48$%) and the standard deviations as dotted lines ($+2.97$% and -2.01%). These figures represent our uncertainty in the description of the water vapour column—in this case, flight A670, we believe the water vapour in our first-guess profile to be

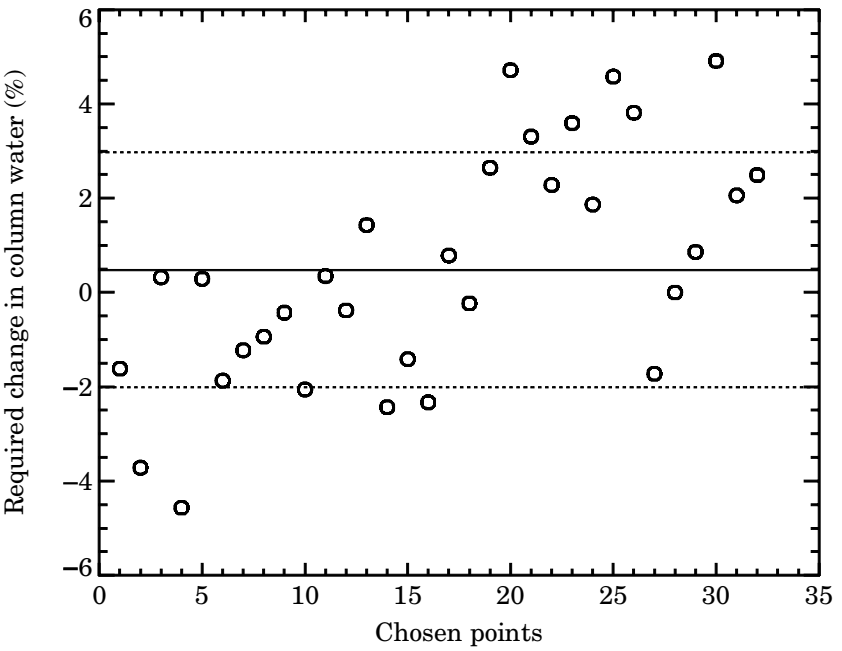

Figure 8. The percentage change in total water vapour column required to force agreement between the ARIES observations and the GENLN2 model simulations for the 32 chosen channels presented in Fig. 7. The horizontal lines show the mean (+0.48%) and standard deviations (+2.97%, −2.01%) of the dataset. See text for details.

within 0.48% of the truth. The atmosphere on this day was particularly uniform in space and time, as was evident from other measurements made with ARIES around the same time and from the AMSU imagery.

Using the results of running GENLN2 with and without the water vapour continuum we have also been able to select those wave numbers where the effects of the water vapour continuum are dominant, i.e. the best 'micro-windows', where water vapour line absorption is negligible. Having estimated our uncertainty in the water vapour column used in the radiation model using spectral positions where the continuum is negligible, it is now constructive to see how these uncertainties translate into the differences observed between observations and models across the wider atmospheric window.

The best-guess profile was modified by +2.97%, +0.48% and −2.01% (these being the mean and standard deviations from our analysis described above), in line with our uncertainty in the water vapour column, to create three new profiles of the atmosphere. These three modified profiles were then input, in turn, to GENLN2 using the CKD2.4 water vapour continuum and the brightness temperature difference between ARIES and GENLN2 studied.

Cormier *et al.* (2002) suggest that the self-broadening coefficient of the water vapour continuum is in error. Using the three modified profiles in the radiance calculation, the self-broadening coefficient of the water vapour continuum has been modified iteratively from that used in the CKD2.4 continuum, until the best agreement between ARIES and GENLN2 simulations are obtained at those spectral points where the continuum dominates and the line absorption is negligible. The result is three modifications to the self-broadening coefficient based on our estimate of the true water vapour profile (first-guess +0.48%) and our uncertainty in this profile (first-guess +2.97% and first-guess −2.01%).

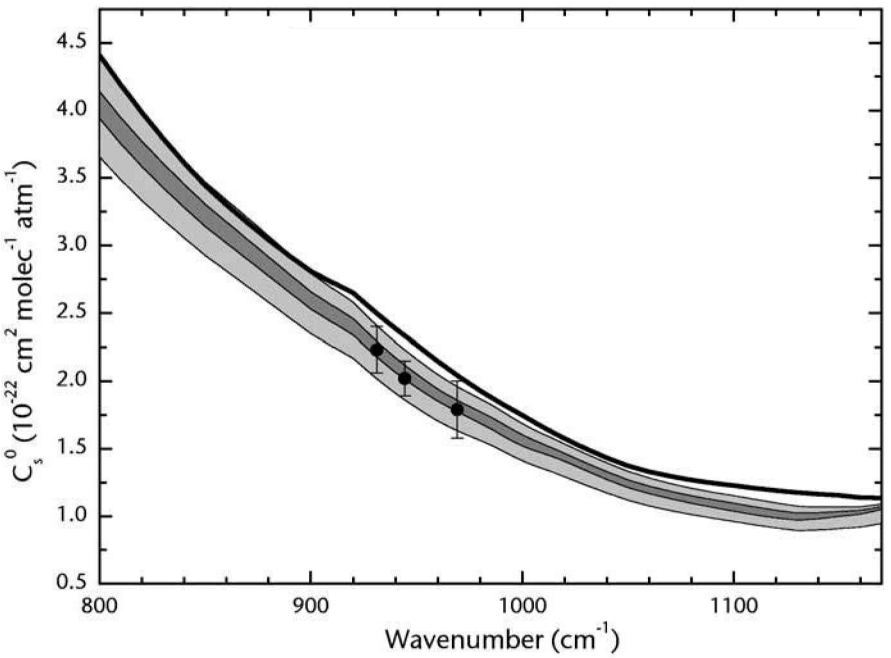

Figure 9. The self-broadening coefficient of the water vapour continuum. The solid line is the standard formulation of the CKD2.4 continuum (see text). The line at the upper edge of the lighter shaded region is the upper bound for the continuum from flight A670. The line at the lower edge of the lighter shaded region is the lower bound for the continuum from flight A676. The darker shaded region indicates the overlap of the analysis for flights A670 and A676. The three data points are the results of Cormier *et al.* (2002) with their associated error bars.

An identical technique has been used to study another flight in the tropics—flight A676 on 6 May 1999. In the same manner as for A670 another set of three modifications to the self-broadening coefficient of the water vapour continuum have been derived.

Figure 9 shows the self-broadening coefficient of the water vapour continuum as a function of wave number. The thick solid line is the value used in CKD2.4. The upper boundary of the light shaded region is inferred from flight A670; the lower boundary of the light shaded region is from A676. The dark shaded region shows the overlap of the results from A670 and A676. The data points and error bars represent the laboratory results from Cormier *et al.* (2002). The analysis of flight A676 showed a larger range of uncertainty in the continuum correction, the first-guess profile needed to be modified by +4.78%, with the uncertainties covering the range +1.42% to +8.02%. This greater spread in the range of continuum needed to find agreement was caused by the larger variability in the atmospheric state observed during the measurement time period. The increased variability in the background atmospheric state on this day was also evident from AMSU satellite imagery.

Figure 9 shows strong evidence, based on two separate flights in tropical conditions, that the water vapour continuum in the thermal infrared window region is too strong. These results support the independent observations of Cormier *et al.* (2002). The best fit to these observations are given in Table 2. Note that for brevity the wave number scale in the table is not regular, with a finer scale only being applied where there is significant structure in the self-broadening coefficients. Linear interpolation between points is sufficient to reconstruct the coefficients.

TABLE 2. BEST ESTIMATE OF THE SELF-BROADENING WATER VAPOUR CONTINUUM TAKING THE AVERAGE OF VALUES DERIVED FROM FLIGHTS A670 AND A676 ARIES SPECTRA

Wave number (cm^{-1})	Self-broadening coefficient, C_s^0 ($cm^2 molec^{-1} atm^{-1} \times 10^{-22}$)	Correction to CKD[1], C_s^0 (this work/CKD 2.4)
800	4.019	0.912
820	3.661	0.919
840	3.354	0.928
860	3.084	0.934
880	2.831	0.931
900	2.581	0.919
910	2.481	0.910
920	2.384	0.901
930	2.237	0.891
940	2.105	0.883
960	1.882	0.877
980	1.720	0.891
1000	1.555	0.890
1020	1.421	0.902
1040	1.290	0.901
1050	1.232	0.897
1060	1.186	0.892
1080	1.117	0.881
1100	1.063	0.866
1120	1.012	0.850
1130	9.918	0.844
1140	9.941	0.854
1160	1.013	0.890
1170	1.041	0.917

[1] See subsection 5(a) and Clough *et al.* (1980, 1989).
The resolution of the data is sufficient for linear interpolation to reproduce the observed wave number dependence (e.g. the resonance between 900 and 940 cm^{-1}). See text for further details.

The corrections to the water vapour continuum have been made solely to the self-broadening coefficients, a reasonable assumption as to the source of the error—other potential sources of error in the continuum, such as temperature dependence, have not yet been evaluated.

The modified continuum was based on zenith observations from low level. In Fig. 10 the nadir measurements made by ARIES over the sea at an altitude of ~8 km during flight A670 are shown with the GENLN2 simulation using the standard CKD2.4 and the modified continuum over the window region between 800 and 1200 cm^{-1}. The atmospheric state was defined using the best profile for this case, i.e. the first-guess profile with the water vapour increased by +0.48%. In Fig. 10(b) broad oscillations in the residual between the observations and calculations are shown. This residual oscillation is removed when the modified continuum is applied (see Fig. 10(c)). This figure shows that the agreement between observation and modelled spectra is improved with the modified continuum.

Between 1010 and 1070 cm^{-1} the difference between the measured and modelled spectra is due to uncertainties in the ozone profile. The ozone profile was based on aircraft measurements up to around 8 km with an ozone sonde for higher levels. However, the ozone sonde measurements were several days previous to the airborne measurements—the reasons for these differences are still being investigated. Between 800 and 1000 cm^{-1} the difference between the model and observations is between 0.1 and 0.2K, which probably equates to the limit of accuracy possible given

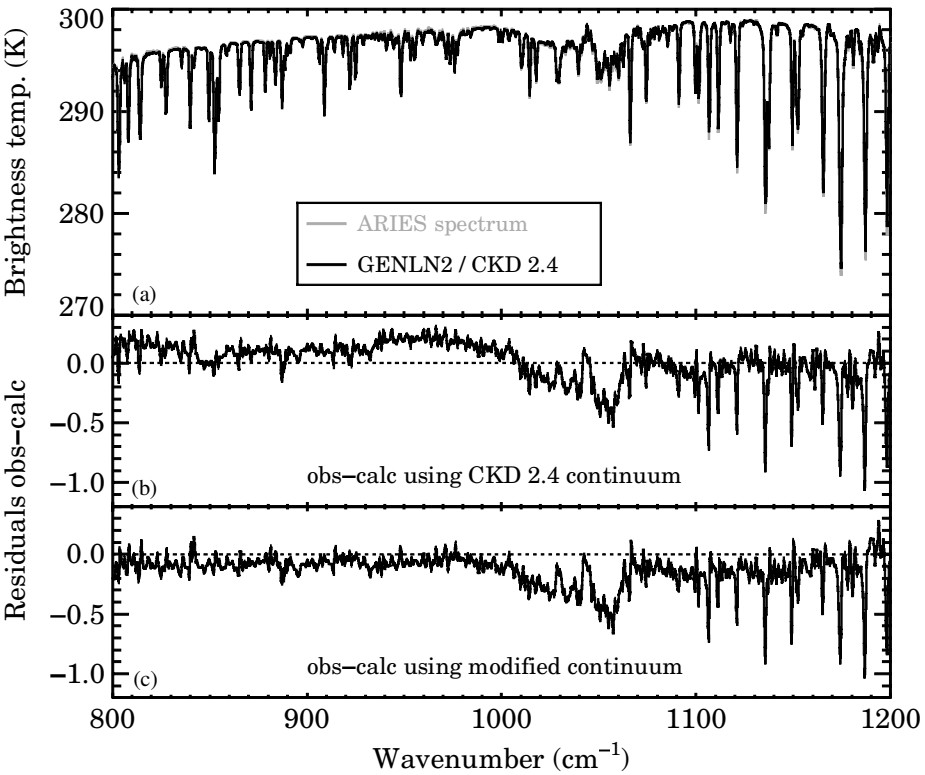

Figure 10. A comparison of ARIES nadir brightness temperature measurements at an altitude of 7.5 km and a GENLN2 simulation during flight A670 in MOTH Tropic: (a) the ARIES observations and GENLN2 model results; (b) and (c) show the difference ARIES minus GENLN2 for the standard CKD2.4 continuum and the modified continuum, respectively. See text for details.

the difficulties in prescribing the true atmospheric state below the aircraft at any one time and the exact sea surface temperature.

The development of a modification to the water vapour continuum was based on two independent flights in the tropics. Figure 11 shows measured and modelled spectra for a case during the MOTH-Arctic experiment. Here the aircraft was flying at an altitude of 9.5 km above the Baltic Sea. The air was coming over the Norwegian and Swedish mountains from the Arctic and was cold and dry. Here the effects of the continuum are very weak since the water vapour column is very low. Figure 11(a) shows the ARIES measurements and GENLN2 simulations; Figs. 11(b) and (c), respectively, show observed minus modelled brightness temperature using the CKD2.4 continuum and the modified continuum based on the corrections given in Table 2. The impact of modifying the continuum is negligible in this cold, dry atmosphere, and the level of agreement between ARIES and the GENLN2 simulations is generally within 0.1—0.2 K. The problem with the definition of the ozone profile remains. Of note is the agreement in the water vapour lines beyond 1000 cm^{-1} which has also improved as a result of the low water vapour amounts.

(*c*) *Sea surface emissivity model*

In modelling the upwelling radiance presented in Fig. 11, the Masuda model of emissivity (Masuda *et al.* 1988) used in GENLN2, was modified. During an aircraft run

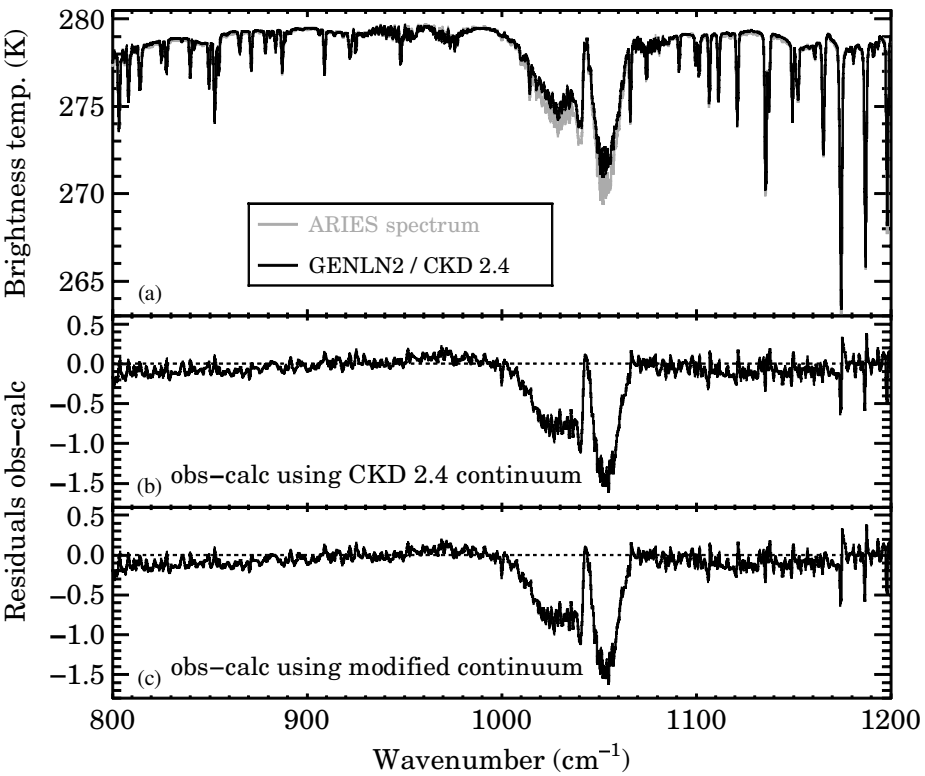

Figure 11. As Fig. 10, but at an altitude of 9.5 km during flight A742 in MOTH Arctic.

at 30 m above the ocean surface the ARIES instrument was directed to make both zenith and nadir views. If the sea surface were black, and there was no intervening atmosphere between the surface and the flight level, then the brightness temperature observed by the ARIES instrument would be constant and representative of the sea surface skin temperature. When looking at data gathered at 30 m it is a reasonable assumption to assume negligible absorption in the window region, except for the strongest water vapour lines. Hence we can use our measured downwelling radiance spectra to infer the reflectance of the ocean surface, since the upwelling spectra is represented by the combination of the surface emitted term and the reflected downwelling term. When this procedure was carried out for low-level data in the tropical oceans, excellent agreement was observed between the Masuda model and the ARIES derived emissivity. However, in the sub-arctic case there were significant differences.

Figure 12 shows the ARIES derived emissivity as the black noisy line—these data have been smoothed and extrapolated, and are shown as the solid grey line. The dashed line is the standard Masuda model, which shows a peak in the emissivity at around 890 cm^{-1}. In order to agree with the ARIES data at low levels we have modified the surface emissivity in GENLN2 from that represented by the Masuda model, by increasing the emissivity slightly in the window region and shifting this peak to around 925 cm^{-1} so as to match the ARIES retrieval at 30 m altitude. Note that the effect of the continuum in the window region between the sea surface and 30 m is negligible. When this modified Masuda emissivity is used within the GENLN2 model in the simulation of the radiances at 9.5 km the level of agreement shown in Fig. 11

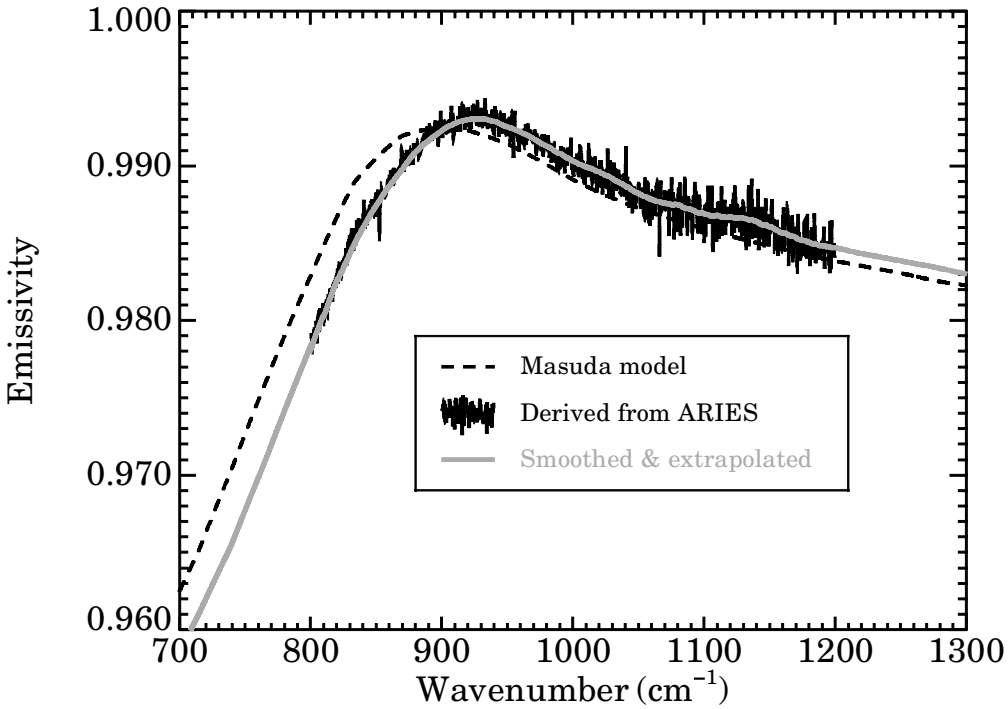

Figure 12. The Masuda model sea surface emissivity for a nadir view over a still ocean (dashed line) with the ARIES derived emissivity (dark line). The ARIES retrieval has been smoothed and extrapolated to a form consistent with the Masuda model (solid light line). See text for details.

is achieved. Without this change to the emissivity, the residual observations minus model brightness temperature shows a wave number dependence, which resembles the difference between the two curves shown in Fig. 12. The modified Masuda model was accepted, since it consistently gave the best agreement with the ARIES observations. Further investigations are being made into the possible reasons for this emissivity difference in sub-arctic waters, which may be related to sea surface temperature or salinity effects.

6. Discussion and conclusions

The role of water vapour in the thermal infrared energy balance of the atmosphere is of critical importance to meteorology and climatology, and the accurate modelling of water vapour spectroscopy is necessary to fully realize the benefit from future high-resolution sounders. The main strengths of the techniques used in this work have been the use of combined infrared and microwave observations utilizing upwelling and downwelling spectral observations at different altitudes to separate possible surface effects and provide columns comprising low and high amounts of water-vapour. In addition, the use of high-spectral-resolution data over a large wavelength range has allowed isolation of spectral regions that are relatively sensitive and insensitive to either water vapour continuum or line parameters.

In this work, analysis of microwave and infrared radiometer data in tropical and sub-arctic atmospheres has been used to assess the uncertainties in water vapour line and continuum absorption. Analysis of data gathered by well characterized microwave

radiometers (McGrath and Hewison 2001) has shown that the spectroscopy around the 183 GHz water vapour line can be well modelled. This has been utilized in defining the first-guess profile for the validation of the infrared models where the spectroscopy is less understood. The synergetic use of microwave and infrared radiometer data allowed greater confidence in our representation of the atmospheric profile in the radiative transfer modelling, and such an approach should be adopted wherever possible. The microwave radiometers flown on the MRF C130 also measured at other frequencies where the microwave continuum is important—these measurements and the uncertainties in the microwave continuum will be detailed elsewhere.

Starting with the first-guess profile based on microwave radiometer data analysis, the most representative atmospheric profile has been built using the high-spectral-resolution data from ARIES. The high-spectral-resolution data, available from interferometers like ARIES, have allowed a detailed analysis of the water vapour continuum in the atmospheric window region between 800 and 1200 cm^{-1} to be conducted. Independent analysis of two flights in the tropical South Atlantic indicated that the CKD2.4 water vapour continuum was too strong and needed to be reduced by a variable amount between 6% and 15%—the exact corrections are available in Table 2. These results are in excellent agreement with the laboratory measurements of Cormier *et al.* (2002) who, for their three spectral points, found the continuum to be too strong and needed to be reduced by 12%. It should be noted that recent independent studies using ground-based interferometer data from the US Department of Energy's Atmospheric Radiation Measurement programme (Turner *et al.* 2004) reach similar conclusions regarding the changes to the self-broadening continuum in the 800–1000 cm^{-1} spectral region. However, our conclusions regarding the 1100–1300 cm^{-1} region do not agree with those of Turner *et al.* (personal communication). They suggest an increase in both the self-broadening and foreign-broadening components of the continuum in this region, whereas we suggest a decrease in the self-broadening component is required.

It is hoped that through studies of data like these, guidance may be given as to the relative confidence in our scientific understanding of various regions of the infrared spectrum. Since space-borne high-resolution sounders like AIRS and IASI have many thousands of channels, careful analysis of the uncertainties in the spectroscopy will help NWP centres in the selection of channels for data assimilation.

Acknowledgements

The authors would like to acknowledge the support of the aircrew and staff of MRF in the MOTH Tropic and Arctic field campaigns, and the excellent ground support offered by the authorities at Ascension Island and Kalmar. The support of the Met Office team from Beaufort Park who launched the supporting radiosondes is also acknowledged. The authors would also like to thank the two referees and the associate editor for their constructive comments.

References

Amato, U., Cuomo, V. and Serio, C. 1995 Assessing the impact of radiometric noise on IASI performances. *Int. J. Remote Sensing*, **16,** 2927–2938

Aumann, H. H. and Pagano, R. J. 1994 Atmospheric infrared sounder on the earth observing system. *Opt. Eng.*, **33,** 776–784

Clough, S. A., Kneizys, F. X., Davies, R. W., Gamache, R. and Tipping, R. 1980 Theoretical line shape for H2O vapour; application to the continuum. Pp. 25–46 in *Atmospheric water vapour*. Eds. A. Deepak, T. D. Wilkerson and L. H. Ruhnke. Academic Press, New York, USA

Clough, S. A., Kneizys, F. X. and Davies, R. W. 1989 Line shape and the water vapour continuum. *Atmos. Res.*, **23,** 229–241

Cormier, J. G., Ciulyo, R. and Drummond, J. R. 2002 Cavity ringdown spectroscopy measurements of the infrared water vapor continuum. *J. Chem. Phys.*, **116,** 1030–1034

Edwards, D. P. 1992 'GENLN2. A general line-by-line atmospheric transmittance and radiance model'. NCAR Technical note NCAR/TN-367+STR, National Center for Atmospheric Research, Boulder, Co., USA

English, S. J., Renshaw, R. J., Dibben, P. C., Smith, A. J., Rayer, P. J., Poulsen, C., Saunders, F. W. and Eyre, J. R. 2000 A comparison of the impact of TOVS and ATOVS satellite sounding data on the accuracy of numerical weather forecasts. *Q. J. R. Meteorol. Soc.*, **126,** 2911–2931

Goodrum, G., Kidwell, K. B. and Winston, W. 2000 'NOAA KLM users guide (September 2000 Revision)'. Available from NOAA at http://perigee.ncdc.noaa.gov/do cs/klm/cover.htm

Han, Y., Shaw, J. A., Churnside, J. H., Brown, P. D. and Clough S. A. 1997 Infrared spectral radiance measurements in the tropical Pacific atmosphere. *J. Geophys. Res.*, **102,** 4353–4356

Liebe, H. J. 1989 MPM—An atmospheric millimeter wave propagation model. *Int. J. Infrared and Millimeter Waves*, **10**(6)**,** 631–650

Liebe, H. J., Hufford G. A. and Cotton, M. G. 1993 'Propagation modeling of moist air and suspended water/ice particles at frequencies below 1000 GHz'. In Proceedings of the NATO/AGARD 52nd Specialists' Meeting of the Electromagnetic Wave Propagation Panel. Paper No. 3/1-10, Palma de Mallorca, Spain

McGrath, A. J. and Hewison T. J. 2001 Measuring the accuracy of a Microwave Airborne Radiometer (MARSS). *J. Atmos. Oceanic Technol.*, **18,** 2003–2012

Masuda, K., Takashima, T. and Takayama, Y. 1988 Emissivity of pure and sea waters for the model sea surface in the infrared window regions. *Remote Sensing Environ.*, **24,** 313–329

Newman, S. M. and Taylor, J. P. 2002 Impact of updates to the HITRAN spectroscopic database on the modeling of clear-sky infrared radiances. *Geophys. Res. Lett.*, **29,** 181–184

Rosenkranz, P. W. 1998 Water vapor microwave continuum absorption: A comparison of measurements and models. *Radio Sci.*, **33,** 919–928

Smith, W. L., Woolf, H. M., Hayden, C. M., Wark, D. Q. and McMillin, L. M. 1979 The TIROS-N operational vertical sounder. *Bull. Am. Meteorol. Soc.*, **60,** 1177–1187

Ström, J., Busen, R., Quante, M., Guillemet, B., Brown, P. R. A. and Heintzenberg, J. 1994 Pre-EUCREX intercomparison of airborne humidity measuring instruments. *J. Atmos. Oceanic Technol.*, **11,** 1392–1399

Vance, A. K., Taylor, J. P. and Hewison, T. J. 2003 Comparison of *in situ* humidity data from aircraft, dropsonde and radiosonde. *J. Atmos. Oceanic Technol.*, in press

Wilson, S. H. S., Atkinson, N. C. and Smith, J. A. 1999 The development of an airborne infrared interferometer for meteorological sounding studies. *J. Atmos. Oceanic Technol.*, **16,** 1912–1927